Optics Communications 317 (2014) 88–92

Contents lists available at ScienceDirect

Optics Communications

journal homepage: www.elsevier.com/locate/optcom

# Effect of the shadowing in high-numerical-aperture binary phase Fresnel zone plates

Yaoju Zhang *, Chongwei Zheng, Youyi Zhuang

*College of Physics and Electronic Information Engineering, Wenzhou University, Wenzhou 325035, China*

ARTICLE INFO

*Article history:*
Received 24 August 2013
Received in revised form
7 October 2013
Accepted 11 October 2013
Available online 27 November 2013

*Keywords:*
Fresnel zone plate
Shadowing
Vector diffraction

ABSTRACT

Shadowing occurs for the groove zone plate when radiation origin from one zone of the zone plate must pass through another before reaching the focus point. Using the vector diffraction theory, we study the influence of the shadowing on the focusing properties of binary phase Fresnel zone plates (FZPs). The results show that a low-numerical-aperture (NA) FZP can be treated as an ideal in-plane FZP and the shadowing effect can be neglected. For a high-NA FZP, however, the shadowing effect from the etch depth has to be considered. Owing to the shadowing, the intensity of focusing spot decreases markedly and the size of focusing spot increases slightly in a high-NA FZP. The optimal etching depth of an actual FZP is smaller than that of an ideal FZP.



## 1. Introduction

The Fresnel zone plate (FZP), an important planar optical element which has lens-like properties, can be used for focusing and imaging electromagnetic waves in a broad spectral range from visible light to X-ray [1–4]. Zone plates accomplish these functions through diffraction and interference, rather than refraction. Recently, microzone plates have been proposed for superfocusing in visible regime [5,6]. Actual high resolution and efficient phase FZPs, which are called as thick FZPs, necessarily must be optically thick and having high aspect ratio (thickness over the zone width). The rigorous calculation of focusing properties for the thick FZP is generally based on solving the parabolic wave equation describing diffraction inside the zone plate body using the finite-difference method [6–8] or using the coupled wave theory [9,10]. In order to ascertain and understand the physics behind the focusing behavior of high numerical aperture (NA) FZPs, Mote et al. developed the vector diffraction theory of Richards and Wolf [11] and analyzed the subwavelength focusing behavior of a high-NA in-plane phase FZP [12]. They found that the analytical results of the normalized intensity distribution in the focal plane are basically same as the rigorous FDTD simulation results. Carretero et al. calculated the near-field focusing of high-NA in-plane subwavelength amplitude FZPs [13,14] using the Luneburg's vector diffraction theory [15] and the vector angular spectrum theory, respectively. They found that the intensity distributions of calculation are a good agreement with the rigorous FDTD simulation results.

A subwavelength FZP, especially a near-field focusing subwavelength phase FZP, is the thick Fresnel zone plate. A thick FZP cannot be treated as the in-plane zone plate (i.e., an amplitude or phase screen) and the effect of the etch depth has to be considered. Shadowing occurs for the groove thick FZP when radiation origin from one zone of the zone plate must pass through another before reaching the focus point. In this paper, the influence of the shadowing zones on the focusing properties of a groove thick FZP is analyzed using the vector diffraction theory of Richards and Wolf [11]. The results show that shadowing has an important influence on the size of the spot intensity in a high-NA thick FZP.

## 2. Shadowing in the binary phase zone plate

Fig. 1 shows the schematic cross section of a binary phase circular thick FZP. The FZP pattern is etched on a dielectric film with diffractive index $n$ and the etch depth is $d$. $f$ is the designed focal length of the primary focus and the origin of coordinates is at the designed focus point. The zone boundaries are written as

$$r_m = \sqrt{mf\lambda + \left(\frac{m\lambda}{2}\right)^2}, \quad m = 1, 2, 3, \cdots, 2N+1, \tag{1}$$

where $2N$ is the zone number of the zone plate.

For the FZP considered in this paper, we assume that the width of the outmost zone is larger than the illumination wavelength so that the coupling effect of lights between groove and ridge zones can be neglected [16,17]. In addition, the designed focal length is much larger than the etching depth of the FZP so that the diffraction inside FZP's body can be neglected. Under these conditions, we can use the ray optics approximation to analyze the propagation of the

* Corresponding author. Tel.: +86 57788752786; fax: +86 57788373109.
*E-mail addresses:* zhangyaoju@sohu.com, zhangyaoju@gmail.com (Y. Zhang).

0030-4018/$ - see front matter © 2014 Published by Elsevier B.V.
http://dx.doi.org/10.1016/j.optcom.2013.10.039

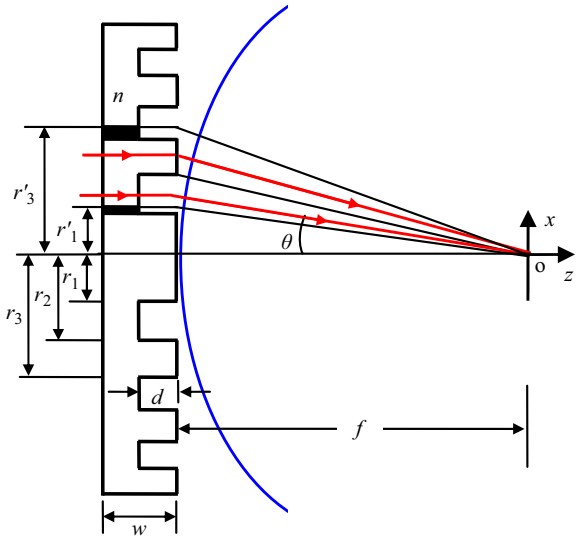


**Fig. 1.** Shadowing geometry in a binary phase zone plate. The black rectangle blocks denote the shadowing zones.

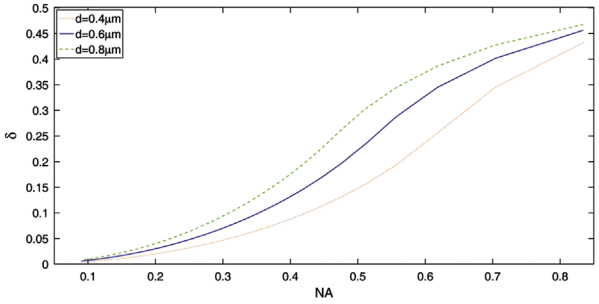


**Fig. 2.** Dependence of the percentage of the shadow area in a binary phase zone plate with $n=1.5426$ and $N=100$ on the numerical aperture for three different values of etch depth. The light with the 405 nm wavelength is normally incident on the FZP.

light within FZP's body. According to the ray optics, shadowing occurs for the groove zone plate when radiation originating from the groove zone of the zone plate must pass through the ridge zone before reaching the focus point, due to the reflection effect. The incident lights within the shadowing zones cannot be converged to the focus point. The black rectangle blocks in Fig. 1 denote the geometry of the shadowing when the light beam is normally incident on the binary phase FZP. It shows that the radiation passing through the odd zones (i.e., groove zones) will be shadowed by the even zones (i.e., ridge zones). The width of each zone that is shadowed is given by $\Delta r_m = d \tan\theta_m$, where $\tan\theta_m$ is equal to $r_m/f$ with $m$ an odd integer. We define the percentage ($\delta$) of shadow area as the ratio between the shadowed area (which is the sum of all the individual shadow zone area) and the entire area on the FZP,

$$\delta = \frac{\pi \sum_{m=1}^{N} (r'^2_{2m-1} - r^2_{2m-1})}{\pi r^2_{2N+1}} \tag{2}$$

where $r'_{2m-1} = r_{2m-1}(1+d/f)$.

Fig. 2 shows the percentage ($\delta$) of shadow area in a binary phase zone plate as a function of the numerical aperture (NA) and etch depth ($d$). It is clear that $\delta$ is larger for larger NA and $d$. For a low-NA FZP, for example, NA $<0.2$, $\delta$ is very small and can be neglected [18]. For a high-NA FZP, for example, NA $>0.6$, $\delta$ is quite large and it has a serious influence on the focusing properties of the zone plate, which will be shown in Section 4.

## 3. Diffraction theory of thick FZPs

For high-NA FZPs where effects due to the vector character of the electric field become important, a vector diffraction theory is necessary. It should be pointed out that the size of the shadow area is associated with the propagation direction of incident light and it is independent of the polarization of incident light. For the considered FZP, we can neglect the coupling effect and diffraction effect inside the FZP. Thus, we continue to use the ray optics method for a vectorial incident beam before lights pass through the FZP but consider the effect of shadowing. After lights pass thought the exit pupil in $z=0$ plane we use the vector diffraction method. In this paper, we assume a linearly unit-amplitude $x$-polarized plane wave is normally incident on a high-NA binary phase FZP. According to the Huygens–Fresnel principle, every point of a wave-front may be considered as a center of a secondary disturbance which gives rise to a spherical wavelet. We can expand this spherical wavelet into an angular spectrum of plane waves [11]. For high-NA FZPs, as in our case, the Debye approximation can be used to calculate this angular spectrum. Only those plane waves, the propagation directions of which correspond to the geometric optical rays, contribute to the field in the focus. In this approximation, diffraction effects due to the edge of the aperture are not considered. The field in the focus can be evaluated by superposing those plane waves, keeping track of the phase and the direction of polarization. Thus, we obtain the components of electric field vector near the focal region [11],

$$\begin{aligned} E_x &= -iA(I_0 + I_2 \cos 2\phi), \\ E_y &= -iAI_2 \sin 2\phi, \\ E_z &= -2AI_2 \cos\phi, \end{aligned} \tag{3}$$

where $A=kfl_0/2$, $l_0$ denotes the relative amplitude of the field and $k=2\pi/\lambda$ is the wave number. $(r, \varphi, z)$ are the cylindrical coordinates at the observed point. $I_0$, $I_1$, and $I_2$ are integrals, given by

$$\begin{aligned} I_0 = &\sum_{m=0}^{N} \int_{\theta_{2m}}^{\theta_{2m+1}} B(\theta) A_r(\theta) \sin\theta (1+\cos\theta) J_0\left(\frac{v \sin\theta}{\sin\alpha}\right) \exp\left(\frac{iu\cos\theta}{\sin^2\alpha}\right) d\theta \\ &+ \sum_{m=0}^{N-1} \int_{\theta'_{2m+1}}^{\theta_{2m+2}} B(\theta) A_g(\theta) \sin\theta (1+\cos\theta) J_0\left(\frac{v \sin\theta}{\sin\alpha}\right) \exp\left(\frac{iu\cos\theta}{\sin^2\alpha}\right) d\theta, \end{aligned} \tag{4}$$

$$\begin{aligned} I_1 = &\sum_{m=0}^{N} \int_{\theta_{2m}}^{\theta_{2m+1}} B(\theta) A_r(\theta) \sin^2\theta J_1\left(\frac{v \sin\theta}{\sin\alpha}\right) \exp\left(\frac{iu\cos\theta}{\sin^2\alpha}\right) d\theta \\ &+ \sum_{m=0}^{N-1} \int_{\theta'_{2m+1}}^{\theta_{2m+2}} B(\theta) A_g(\theta) \sin^2\theta J_1\left(\frac{v \sin\theta}{\sin\alpha}\right) \exp\left(\frac{iu\cos\theta}{\sin^2\alpha}\right) d\theta, \end{aligned} \tag{5}$$

$$\begin{aligned} I_2 = &\sum_{m=0}^{N} \int_{\theta_{2m}}^{\theta_{2m+1}} B(\theta) A_r(\theta) \sin\theta (1-\cos\theta) J_2\left(\frac{v \sin\theta}{\sin\alpha}\right) \exp\left(\frac{iu\cos\theta}{\sin^2\alpha}\right) d\theta \\ &+ \sum_{m=0}^{N-1} \int_{\theta'_{2m+1}}^{\theta_{2m+2}} B(\theta) A_g(\theta) \sin\theta (1-\cos\theta) J_2\left(\frac{v \sin\theta}{\sin\alpha}\right) \exp\left(\frac{iu\cos\theta}{\sin^2\alpha}\right) d\theta, \end{aligned} \tag{6}$$

where $\theta$ is the angle between a diffracted ray and the optical axis. $\alpha = \arctan(r_{2N+1}/f)$, $\theta_j = \arctan(r_j/f)$, and $\theta'_j = \arctan[(r_j+\Delta r_j)/f]$ where $\Delta r_j = r_j d/f$ is the width of the shadowing in the $j$th zone and $j$ is an odd number. $J_m(\rho)$ is the Bessel function of the first kind and $m$ is the order of the Bessel function. $u=kz\sin^2\alpha$ and $v=kr\sin\alpha$ are the normalized cylindrical coordinates. $B=\cos^{-3/2}\theta$ is the apodization factor for a diffractive zone plate [19,20]. $A_r$ and $A_g$ are the aberration functions of lights from the ridge and groove zones, respectively,